ELSEVIER

Journal of Fluids and Structures 22 (2006) 819–827

JOURNAL OF FLUIDS AND STRUCTURES

www.elsevier.com/locate/jfs

Experimental investigation of flow-induced vibration interference between two circular cylinders

G.R.S. Assi[a], J.R. Meneghini[a,*], J.A.P. Aranha[a], P.W. Bearman[b], E. Casaprima[c]

[a]*NDF, "Escola Politécnica", Department of Mechanical Engineering, University of São Paulo, CEP 05508-900 São Paulo, SP, Brazil*
[b]*Department of Aeronautics, Imperial College, London SW7 2BY, UK*
[c]*Petrobras, CENPES, Rio de Janeiro, Brazil*

Received 1 October 2005; accepted 9 April 2006
Available online 24 July 2006

Abstract

This paper presents experimental results concerning flow-induced oscillations of circular cylinders arranged in tandem. New measurements on the dynamic response oscillations of an isolated cylinder and flow interference of two cylinders are shown. Preliminary flow visualization employing a PIV system is also shown. The models are mounted on an elastic base fitted with flexor blades and instrumented with strain gauges. The base is fixed on the test-section of a water channel facility. The flexor blades possess a low-damping characteristic ($\zeta \simeq 0.008-0.0109$) and they are free to oscillate only in the cross-flow direction. The Reynolds number of the experiments is from 3000 to 13 000, and reduced velocities, based on natural frequency in still water, vary up to 12. The interference phenomenon on VIV is investigated by conducting experiments in which the upstream cylinder is maintained fixed and the downstream one is mounted on the elastic base. The results for an isolated cylinder are in accordance with other measurements found in the literature for $m^* \simeq 2$ and 8. For the tandem arrangement and $m^* \simeq 2$, the trailing cylinder oscillation presents what previous researchers have termed interference galloping behaviour for a centre-to-centre gap spacing ranging from $2D$ to $5.6D$. These initial results validate the experimental set-up and lead the way for future work, including tandem, staggered and side-by-side arrangements with the two cylinders free to move.

Keywords: Vortex-induced vibration; Flow interference; Vortex shedding

1. Introduction

Flow interference among groups of cylinders has been the subject of many studies in the past. The interference is responsible for several changes in the characteristics of fluid loads when more than one body is placed in a fluid stream. Investigations of the flow around pairs of cylinders can provide a better understanding of the vortex dynamics, pressure distribution and fluid forces, in cases involving more complex arrangements.

This paper presents an experimental study of the flow interference between a pair of rigid cylinders, in tandem configurations, with the rear cylinder elastically mounted and free to oscillate transversely to the flow. In addition, it presents new measurements for an isolated rigid cylinder. In all cases the cylinders are allowed to oscillate only in the

*Corresponding author. Tel.: +55 11 3091 5641; fax: +55 11 3091 5642.
E-mail address: julio.meneghini@poli.usp.br (J.R. Meneghini).

0889-9746/$ - see front matter © 2006 Elsevier Ltd. All rights reserved.
doi:10.1016/j.jfluidstructs.2006.04.013

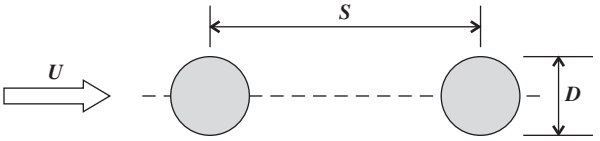

Fig. 1. Configuration for the tandem arrangement.

transverse direction. Dynamic response and forced oscillations of an isolated cylinder have been carefully studied through the past years. Detailed information and accurate data are found in many reviews and recent studies: Bearman (1984), Blevins (1990), Khalak and Williamson (1996, 1999), Krishnamoorthy et al. (2001), and Williamson and Govardhan (2004) among others. Recently, new studies have been published focusing on understanding vortex-suppressor devices, as presented by Bearman and Branković (2004) and Owen et al. (2001).

Many of the previous works regarding the flow around two circular cylinders identified various *interference regimes* and were based primarily on flow visualization in experiments. Investigations such as those by Igarashi (1981), Zdravkovich (1977, 1987) and Sumner et al. (2000) proposed classifications of these regimes. Quoting Zdravkovich, "when more than one bluff body is placed in a fluid flow, the resulting forces and vortex shedding pattern may be completely different from those found on a single body at the same Reynolds number." A variety of flow patterns, characterized by the behaviour of the wake region, may be discerned as the centre-to-centre spacing between two circular cylinders (gap S) is varied; see Fig. 1. The phenomenon has also been intensely analysed by numerical methods, as seen in Meneghini et al. (2001), for instance.

Some results about flow interference between a pair of cylinders in tandem can also be found in the investigations by King and Johns (1976), Bokaian and Geoola (1984), Brika and Laneville (1997, 1999), and Hover and Triantafyllou (2001). All these papers present experimental results of a trailing rigid cylinder oscillating in the wake of an upstream one. According to Bokaian and Geoola (1984), in the case of a fixed leading cylinder, both vortex-resonance and wake galloping instability phenomena are relevant and can occur separately or combined, depending on the separation distance. For $7 \leqslant S/D \leqslant 8.5$, Brika and Laneville (1999) observed that the downstream cylinder exhibited a combination of galloping and vortex-induced vibration.

This paper presents new measurements of vortex-induced vibration of a single cylinder. The experiments are carried out in order to validate the experimental set-up and data processing for future investigations. In addition, they introduce the base results for comparisons with induced oscillations of a trailing rigid cylinder in a tandem arrangement. A brief description of the apparatus and some remarks regarding future investigations complements the material. Some preliminary PIV flow visualization techniques are shown for two fixed cylinders arranged in tandem.

2. Experimental set-up

Tests were conducted at the Hydrodynamics Laboratory of Imperial College (IC), London, and at the Fluid-Dynamics Research Group Laboratory of the University of São Paulo (USP). The circulating water channel facility at IC had a $0.60 \times 0.70 \times 8.00$ m test-section, and the facility at USP had a $0.70 \times 0.80 \times 7.50$ m test-section. Both could operate at good quality and well-controlled flows up to 0.7 m/s. Rigid cylinder models were made of aluminium tubes with diameter $D = 32$ mm and wet-length $L = 560$ mm under the water level. Cylinders were vertically clamped by their upper end at the bottom block of elastic supports (firmly fixed on the channel structure) and terminated at their lower end with a 2.0 mm gap on to the test-section floor. The open section channel facilities at IC and USP were equipped with glass walls and a glass floor offering a complete view of the models. For tandem arrangements, the gap between the cylinder centres varied through four different discrete displacements: $S/D = (2.0, 3.0, 4.0, 5.0, 5.6)$. Fig. 2 presents a schematic cross-sectional view of the apparatus mounted on the channel structure.

Both cylinders were independently mounted under an individual elastic base free to oscillate transversely to the flow direction, i.e., only in the cross-flow direction. For each flexible base system, the transverse degree of freedom could be locked, so every model could or could not be free to move in cross-flow oscillations, resulting in different tandem oscillating configurations. Both elastic systems were built with two parallel rigid aluminium blocks, coupled by a pair of thin spring-steel blade flexors. These bases not only act as the cylinder support, but also provide the restoration system response. This flexion-based arrangement was confirmed as a low-damping elastic system. In order to measure cylinder displacements, four strain gauges were built in each pair of blades close to the highest bending region of the face. A complete bridge was built up enabling a linear cylinder displacement signal to be acquired. A set of three base systems was available for isolated cylinder experiments, while another two systems were prepared for tandem arrangement tests.

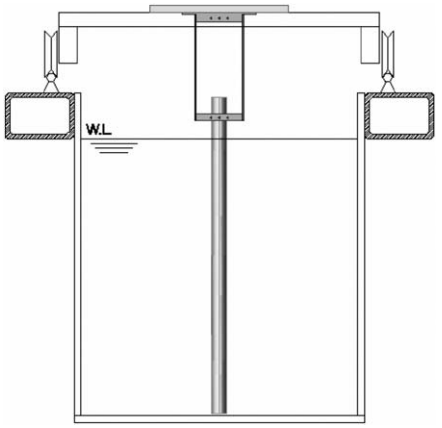

Fig. 2. Cylinder and elastic base mounted on the channel test-section structure.

Table 1
Oscillation parameters for the bases tested

Base identification	m^*	f_N	ζ	$m^*\zeta$
Single cylinder (low mass IC)	0.96	1.56	0.008	0.008
Single cylinder (low mass USP)	0.90	1.17	0.0109	0.010
Single cylinder (median mass IC)	1.92	0.98	0.007	0.013
Single cylinder (high mass IC)	8.06	1.17	0.002	0.016
Pair: downstream cylinder (IC)	1.92	0.98	0.007	0.013
Pair: downstream cylinder (USP)	0.90	1.17	0.0109	0.010

The different bases providing different mass ratios. Mass ratio and spring stiffness were the structural parameters that were varied. Table 1 lists the oscillation parameters obtained for all those configurations. Models tested at Imperial College are indicated by IC, and those models tested at the University of São Paulo are indicated by USP.

Decay tests in water were employed to obtain the natural oscillation frequency (f_N), while the structural damping parameter (ζ) was obtained from decay test performed in air. Mass ratio (m^*) is defined as $m^* = 4M/\rho\pi D^2 L$ (where M represents the total oscillating mass and ρ is the water density). The added mass has not been considered in this definition. Fig. 3 details the elastic base and its spring blades (cross-flow direction is identified by the y-axis) and Fig. 4 shows the experimental apparatus installed in the channel test-section.

3. Results and discussion

The dynamic responses of the models are described in terms of reduced amplitude A/D versus reduced velocity V_r. Some results found in the literature are shown for comparison. Amplitude peaks were calculated employing the Hilbert transform, as described in Khalak and Williamson (1999). Reynolds number (calculated for a single cylinder with diameter D and current velocity U) ranges from $\mathrm{Re} = 3000$ and 13 000 in all experiment cases. The reduced velocity $V_r = f_N U/D$ range extended to a maximum value of 12, hence covering the occurrence of several possible phenomena.

3.1. Single circular cylinder

The responses for an isolated cylinder, with three values of mass and damping parameters, are shown in Figs. 5, Fig. 6, and Fig. 7. These three figures compare the present data to results found in the literature for the three different conditions mentioned before: low mass, median mass, and high mass. They are employed as a baseline for comparisons with the tandem arrangement cases. The following series presents the dynamic response of a single cylinder, free to oscillate in the cross-flow direction, mounted on a low-damping elastic system. In Fig. 5, the nondimensional amplitude of oscillation is presented versus the reduced velocity for $m^* \simeq 1$. The current speed was increased in order to obtain this

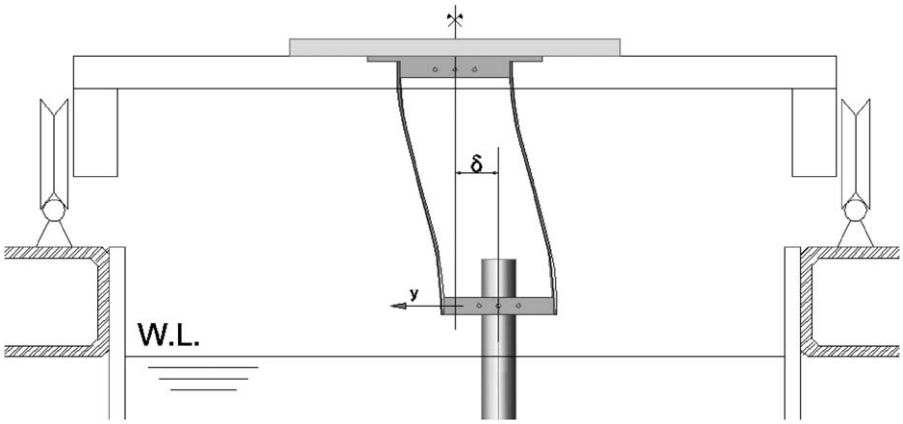

Fig. 3. Detail of the elastic base at a flexing instant. W.L. represents the water line level and δ the horizontal displacement of the cylinder centre.

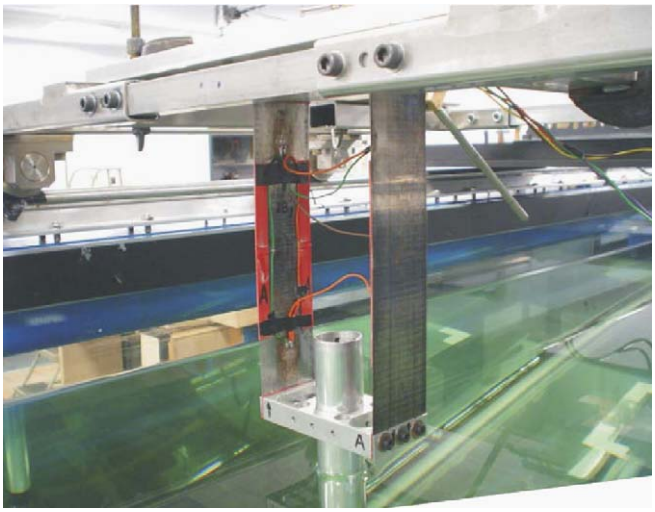

Fig. 4. Cylinder and elastic base mounted on the channel test-section structure.

curve. Our maximum amplitude for the IC model is slightly below $1D$ and it occurs at a reduced velocity $V_r \simeq 6$. The maximum amplitude for the USP model is about $1.2D$ and it takes place at about the same reduced velocity. Our results compare relatively well with those obtained by Branković (2004), in which the reduced velocity range was extended up to 14. For this low mass parameter case, one can notice that oscillation starts at about $V_r \simeq 2.5$ and is sustained up to very high reduced velocity. Such behaviour is expected for very low mass parameter experiments and has already been observed in other investigations. For the low mass parameter model in the IC experiment, the maximum reduced velocity tested could not be increased beyond $V_r = 7$ due to the low stiffness of the flexor blades. In order to increase the in-line stiffness of the base, a third flexor blade has been added to the models tested at USP, which allowed higher velocities to be tested. For this model, reduced velocities up to 12 have been tested.

Fig. 6 shows the response for $m^* \simeq 2$. In this case, we compare our results with those by Khalak and Williamson (1999), and Hover and Triantafyllou (2001). Although the experimental apparatuses used were based on different concepts, the mass and damping parameters are very similar and the observed responses are in close agreement. The oscillations start at about $V_r \simeq 3.0$ and are sustained up to $V_r = 12.0$. The peak amplitude in the present investigation is around $0.9D$. Finally, in Fig. 7, the results for $m^* \simeq 8$ are shown and compared to those by Khalak and Williamson (1999) and Fujarra (2002). The oscillation starts at about $V_r \simeq 3.5$ and the peak amplitude observed in the present results is around $1D$.

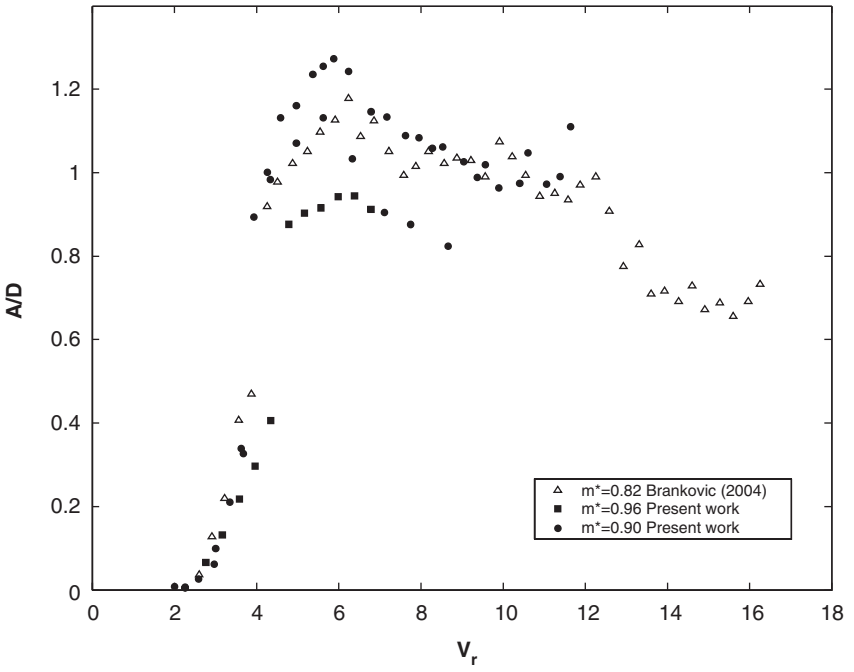

Fig. 5. Variation of the reduced amplitude A/D versus reduced velocity V_r for an isolated cylinder with low mass ratio parameter. Present work: ■, IC model, $m^* = 0.96$, $(m^*\zeta) \simeq 0.008$; •, USP model, $m^* = 0.90$, $(m^*\zeta) \simeq 0.010$; △, Branković (2004), $m^* = 0.82$, $(m^*\zeta) \simeq 0.0001$.

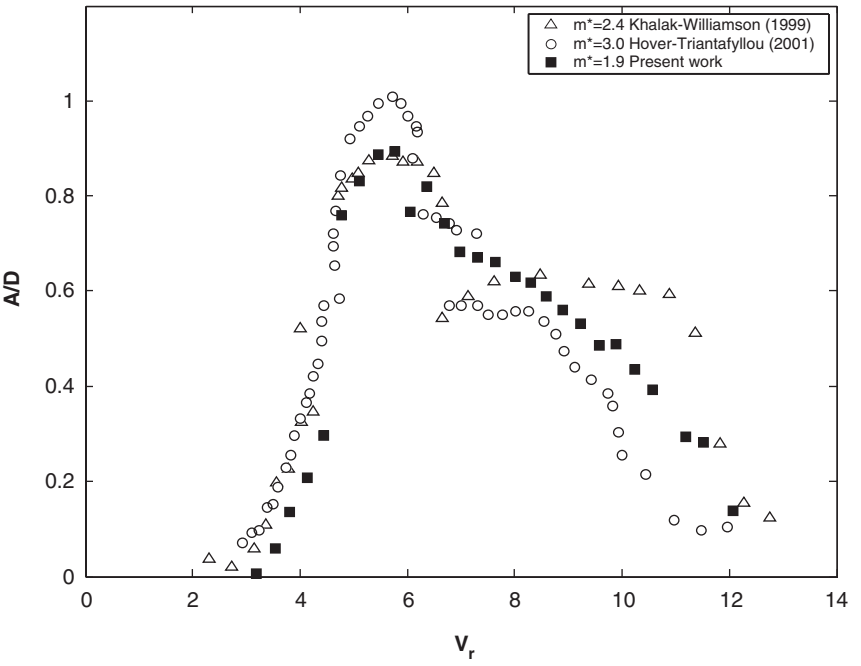

Fig. 6. Variation of the reduced amplitude A/D versus reduced velocity V_r for an isolated cylinder with the median mass ratio parameter. Present work: ■, $m^* \simeq 2$, $(m^*\zeta) \simeq 0.013$; △, Khalak and Williamson (1999), $m^* \simeq 2$, $(m^*\zeta) \simeq 0.014$; ○, Hover and Triantafyllou (2001), $m^* \simeq 3$.

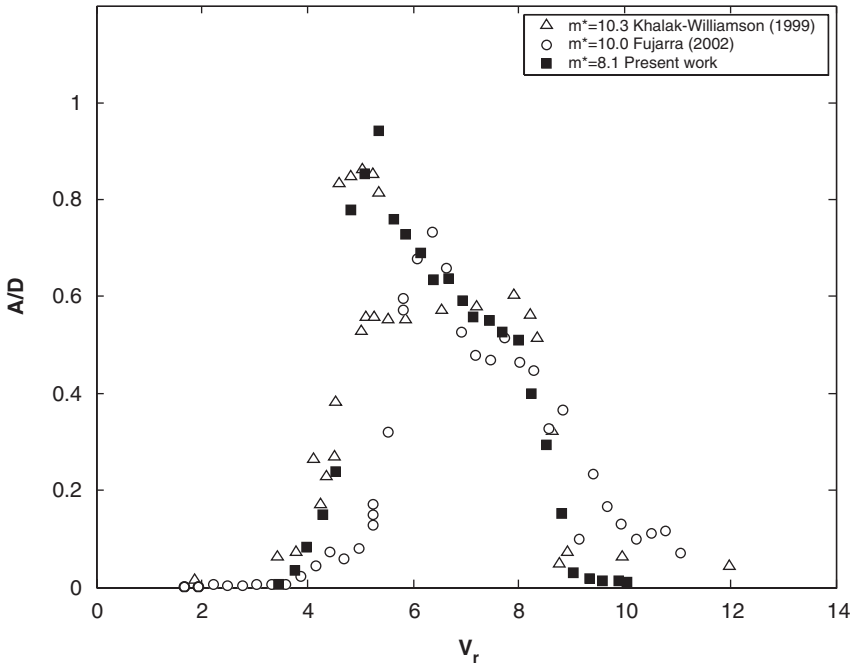

Fig. 7. Variation of the reduced amplitude A/D versus reduced velocity V_r for an isolated cylinder with the highest mass ratio parameter. Present work: ■, $m^* \simeq 8$, $(m^*\zeta) = 0.016$; △, Khalak and Williamson (1999), $m^* \simeq 10$, $(m^*\zeta) \simeq 0.017$; ○, Fujarra (2002), $m^* \simeq 10$, $(m^*\zeta) \simeq 0.03$.

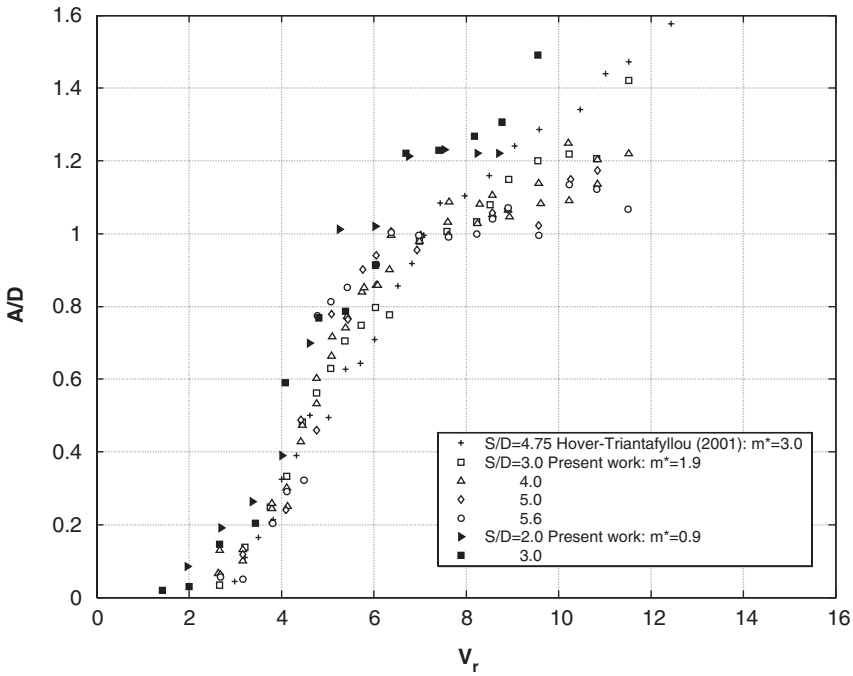

Fig. 8. Variation of the reduced amplitude versus A/D reduced velocity V_r for the trailing cylinder of a pair in tandem arrangement. Present work: □, △, ◇, ○, IC model, $m^* \simeq 2$, $(m^*\zeta) = 0.013$; ■, ▲, USP model, $m^* = 0.9$, $(m^*\zeta) = 0.010$; *, Hover and Triantafyllou (2001), $m^* \simeq 3$.

3.2. Two circular cylinders in tandem

Fig. 8 presents the dynamic results for flow interaction of a trailing rigid cylinder oscillating in the wake of a fixed leading one. The downstream body is free to move only in the cross-flow direction. For this case, $m^* \simeq 2$ and $m^*\zeta \simeq 0.013$. The results are compared with those obtained by Hover and Triantafyllou (2001) with a cylinder with a slightly higher mass parameter. The distance S/D is measured centre to centre. The results shown in Fig. 8 are for four gaps: $S/D = 2.0$, 3.0, 4.0, 5.0, and 5.6. For each gap the response is found to be a monotonically increasing curve without an upper and lower branch typical of an oscillating single cylinder. This continuous increase in the response with increasing reduced velocity is usually found in galloping like- oscillations. To verify this galloping behaviour, higher reduced velocity tests are planned.

The oscillation starts at about $V_r = 2.5$ and grows continuously. The peak amplitude in our experiment is about $1.4D$, which is 50% higher than the maximum amplitude observed for the isolated cylinder case. This peak occurred for the maximum reduced velocity that could be reached by the water channel, i.e., $V_r = 12$. This peak amplitude of the downstream cylinder is observed for a gap $S/D = 3$. It is interesting to note that this increase in amplitude is not observed in interference experiments carried out in air at a higher mass ratio, as reported by Brika and Laneville (1999). Although they observed a continuous response curve, the amplitude reached a maximum similar to the case of an

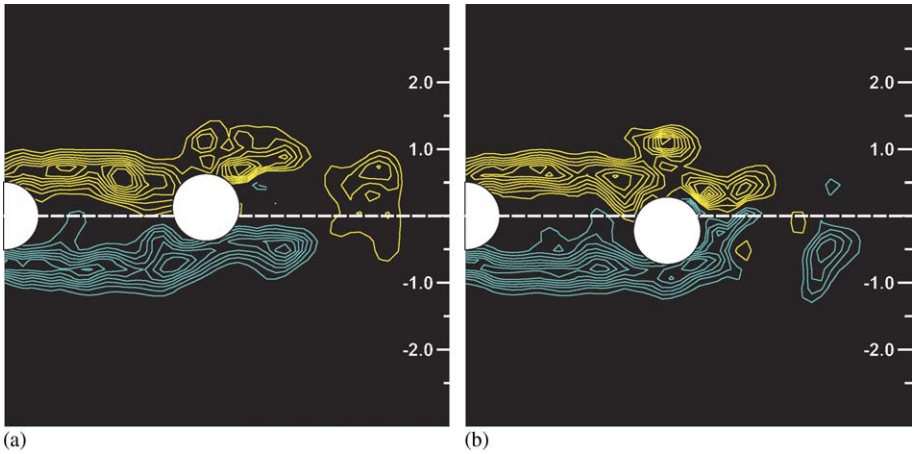

Fig. 9. Flow visualizations employing a PIV system, two cylinders in tandem, $S/D = 3.0$, $\mathrm{Re} = 3200$, $V_r = 2.6$, $A/D \simeq 0.2$; downstream cylinder at (a) uppermost position and (b) lowermost position.

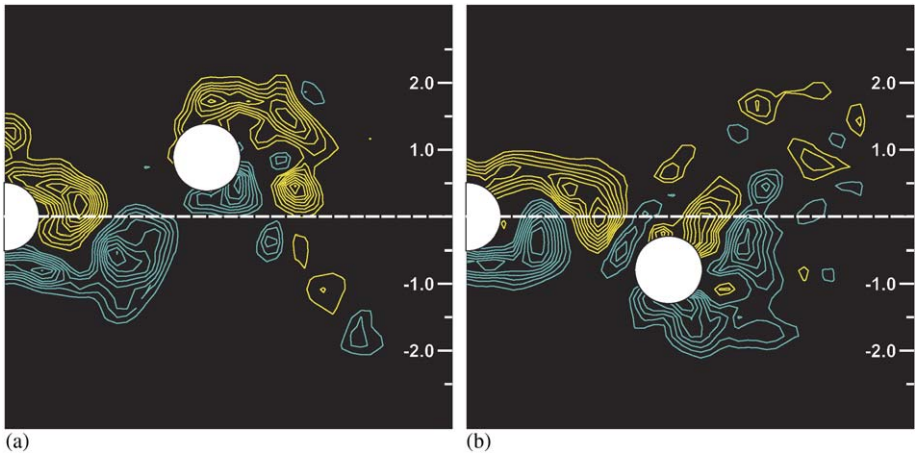

Fig. 10. Flow visualizations employing a PIV system, two cylinders in tandem, $S/D = 3.0$, $\mathrm{Re} = 7300$, $V_r = 6$, $A/D \simeq 0.9$; downstream cylinder at (a) uppermost position and (b) lowermost position.

isolated cylinder. As one can see in Fig. 8, the response of the downstream cylinder at $V_r = 12$ decreases slowly with increasing gap spacing. For $S/D = 5.6$, the largest gap spacing tested, the influence of the upstream cylinder is still pronounced.

Finally, flow visualizations of the USP model, employing a PIV system, are shown in Figs. 9 and 10. The case for a gap $S/D = 3$ is considered, and the vorticity contours are shown when the oscillating downstream cylinder is at its uppermost and lowermost positions. Fig. 9 shows the results for $V_r = 2.6$ and Fig. 10 the results for $V_r = 6.0$. In the first case, the maximum amplitude is slightly below $0.2D$, and the flow visualization shows that the shear layers roll up after the downstream body. Although the second body is oscillating with low amplitude, the cylinders almost behave as a single body, and vortex shedding does not occur in the gap region. In the case for $V_r = 6.0$, vortex shedding occurs in-between the cylinders and the shedding is synchronized with the oscillation. The amplitude of oscillation, for this reduced velocity, is about $0.9D$. Fig. 10 clearly shows that when the cylinder is at its uppermost position, a counterclockwise vortex shed from the upstream cylinder passes close to the lower half of the downstream cylinder. This will create a low-pressure region which acts to pull the cylinder downwards. Whether similar behaviour is observed for higher reduced velocities is still unknown. In the next phase of the current research, PIV images will be employed to investigate such cases.

Despite the fact that the amplitude response curve is similar to galloping, new measurements and CFD calculations suggest that the transverse forces on the downstream cylinder are due to vortex shedding and they are enhanced by vortices coming from the upstream cylinder. Therefore, a better term to illustrate the observed behaviour would be WIV, *wake-interference vibrations*, which describes the phenomenon responsible for these excitations and combines: lock-in of shedding frequency from VIV and interference from the vortices shed from the upstream body.

4. Conclusions

The results for an isolated cylinder were found to be in accordance with other reported measurements for $m^* \simeq 1$, 2, and 8. Consequently, the results are satisfactory to validate the experimental set-up. The decay tests performed in air verified the low-damping behaviour of the base. For the tandem configuration ($m^* \simeq 1$ and 2), one can notice a predominance of the galloping-like phenomenon for the gap range $3.0 < S/D < 5.6$, since the amplitude curve does not show a peak response, and increases continuously with increasing reduced velocity. Higher reduced velocity experiments are planned to be carried out to confirm such behaviour. The peak amplitude observed for the downstream cylinder was about 50% higher than the one observed for the isolated cylinder case. The experiments shown in this paper are still preliminary and are part of an ongoing research project. Future investigations will include tandem, staggered and side-by-side arrangements with the two cylinders free to move.

Acknowledgements

The authors gratefully acknowledge the support by FINEP/CTPetro, FAPESP, CNPq and Petrobras, for providing a research grant for this investigation. The first author is also grateful to FAPESP for his MSc research grant. Special thanks are due to Maša Branković, from Imperial College, London (where part of the experiments were conducted), for her valuable help. The comments and suggestions made by Profs André L.C. Fujarra, Fábio Saltara, Clóvis A. Martins, and Celso P. Pesce are greatly appreciated.

References

Bearman, P.W., 1984. Vortex shedding from oscillating bluff bodies. Annual Review of Fluid Mechanics 16, 195–222.

Bearman, P.W., Branković, M., 2004. Experimental studies of passive control of vortex-induced vibration. European Journal of Mechanics B: Fluids 23, 9–15.

Blevins, R.D., 1990. Flow-Induced Vibration, second Edition. Van Nostrand Reinhold, New York.

Bokaian, A., Geoola, F., 1984. Wake-induced galloping of two interfering circular cylinders. Journal of Fluid Mechanics 146, 383–415.

Branković, M., 2004. Vortex-induced vibration attenuation of circular cylinders with low mass and damping. Imperial College, University of London, London, UK.

Brika, D., Laneville, A., 1997. Wake interference between two circular cylinders. Journal of Wind Engineering and Industrial Aerodynamics 72, 61–70.

Brika, D., Laneville, A., 1999. The flow interaction between a stationary cylinder and a downstream flexible cantilever. Journal of Fluids and Structures 13, 579–606.

Fujarra, A.L.C., 2002. Estudos experimentais e analíticos das vibrações induzidas pela emissão de vórtices em cilindros flexíveis e rígidos. Ph.D. Thesis, Escola Politécnica da Universidade de São Paulo, São Paulo, Brazil.

Hover, F.S., Triantafyllou, M.S., 2001. Galloping response of a cylinder with upstream wake interference. Journal of Fluids and Structures 15, 503–512.

Igarashi, T., 1981. Characteristics of the flow around two circular cylinders arranged in tandem. Bulletin of JSME 24 (188), 323–331.

Khalak, A., Williamson, C.H.K., 1996. Dynamics of a hydroelastic cylinder with vey low mass and damping. Journal of Fluids and Structures 10, 455–472.

Khalak, A., Williamson, C.H.K., 1999. Motions, forces and mode transitions in vortex-induced vibrations at low mass-damping. Journal of Fluids and Structures 13, 813–851.

King, R., Johns, D.J., 1976. Wake interaction experiments with two flexible cylinders in flowing water. Journal of Sound and Vibration 45, 259–283.

Krishnamoorthy, S., Price, S.J., Païdoussis, M.P., 2001. Cross-flow past an oscillating circular cylinder: Synchronization phenomena in the near wake. Journal of Fluids and Structures 15, 955–980.

Meneghini, J.R., Saltara, F., Siqueira, C.L.R., Ferrari Jr., J.A., 2001. Numerical simulation of flow interference between two circular cylinders in tandem and side-by-side arrangements. Journal of Fluids and Structures 15, 327–350.

Owen, J.C., Bearman, P.W., Szewczyk, A.A., 2001. Passive control of VIV with drag reduction. Journal of Fluids and Structures 15, 597–605.

Sumner, D., Price, S.J., Païdoussis, M.P., 2000. Flow-pattern identification for two staggered circular cylinders in cross-flow. Journal of Fluid Mechanics 411, 263–303.

Williamson, C.H.K., Govardhan, R., 2004. Vortex-induced vibrations. Annual Review of Fluid Mechanics 36, 413–455.

Zdravkovich, M.M., 1977. Review of flow interference between two circular cylinders in various arrangements. ASME Journal of Fluids Engineering 99, 618–633.

Zdravkovich, M.M., 1987. The effects of interference between circular cylinders in cross flow. Journal of Fluids and Structures 1, 239–261.